

Numerical and Experimental Investigation of Convex Laser Forming Process

Wenchuan Li and Y. Lawrence Yao, Dept. of Mechanical Engineering, Columbia University, New York, New York, USA. E-mail: yly1@columbia.edu

Abstract

Laser forming is a flexible sheet metal forming technique using laser-induced thermal deformation to shape sheet metal without hard tooling or external forces. Concave laser forming can be readily achieved, while convex forming may occur through buckling, but the buckling direction heavily depends on the sheet surface and pre-strain condition. A new laser scanning scheme is postulated, by which convex forming can be effected insensitive to the abovementioned disturbances. The postulate is successfully validated by experimental and numerical results. The effect of the scanning parameters on the certainty of the convex forming, and dependencies of bend angle on Fourier number, laser power, and dimensionless velocity, are further investigated experimentally and numerically. The simulation results are in agreement with experimental observations. The numerical simulation model developed is also used to study the transient temperature, stress state, and strain state and to provide further insight into the convex forming process.

Keywords: Laser Forming, Nontraditional Manufacturing, Sheet Metal, Finite Element Analysis

Introduction

The laser forming process uses laser-induced thermal distortion to shape sheet metal without hard tooling or external forces. A majority of work on laser forming to date has been based on the so-called temperature gradient mechanism (TGM) proposed by Vollertsen.¹ Under TGM, the workpiece always bends concavely (bends toward the irradiated surface or toward the laser beam). Analytical and numerical modeling efforts have been made for the TGM-dominated laser forming process, which is fairly well understood.¹⁻⁶

However, there are occasions in practical applications where convex forming is required. *Figure 1* shows an example where concave laser bending cannot be applied due to impossible access by the laser beam. It has been shown that convex bending is possible under the buckling mechanism (BM). When

the ratio of laser beam diameter to sheet thickness is large, the through-thickness temperature gradient is lower. The thermal expansion, which is more or less uniform throughout the sheet thickness, is constrained by the surrounding material. As a result, the buckling of the heated metal occurs.⁷

Understandably, the direction of the buckling heavily depends on the sheet conditions, including surface finish and pre-strain/stress. For example, if a sheet is slightly bent, the buckling will most likely take place in the bent direction. In fact, Arnet and Vollertsen⁷ conducted research on convex bending using slightly pre-bent sheets. They experimentally investigated dependency of bend angle on laser power, scanning velocity, and beam diameter for steel (St14), AlMg3, and Cu at different values of thickness. They also conducted a well-known experiment in which unbent but heavily constrained samples were used to demonstrate the existence of the buckling mechanism and the feasibility of convex bending under the condition. The sample is mechanically constrained at both ends instead of clamping on one side only. Holzer and Geiger⁸ conducted a numerical simulation under a similar condition.

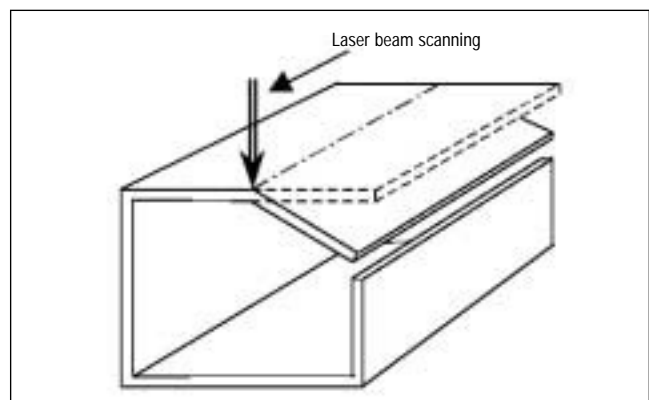


Figure 1
Example Requiring Convex Forming
(dash lines indicating the shape before laser forming)

Vollertsen and Kals⁹ proposed an analytical model for laser forming under the buckling mechanism. An expression for the final bending angle was obtained using the elementary theory of bending and a qualitative model proposed:

$$\alpha_b = \left[36\alpha_{th}k_f A_p / c_p \rho E v s^2 \right]^{1/3}$$

where α_{th} is the coefficient of thermal expansion, k_f the flow stress in the heated region, A_p the coupled laser power, c_p the specific heat of the material, ρ the density, E the modulus of elasticity, v the processing speed, and s the sheet thickness. The model does not determine the direction of the buckling.

For industrial applications, pre-bending a flat workpiece or heavily constraining a sheet to effect convex bending is not economical for obvious reasons and sometimes is impossible, as seen in *Figure 1*. It is postulated that, under the process condition of buckling, if the starting point of the laser scan is at a point other than one on a sheet edge, the direction of buckling will be certain, that is, convex. In almost all laser forming work reported to date, the scan starts from an edge of the sheet. The postulate is based on the fact that although the temperature difference between the top and bottom surface is small under the buckling mechanism, the flow stress is slightly lower, and the tendency of thermal expansion is slightly higher at the top surface because of the slightly higher temperature there.⁹ The slight difference will be amplified by the heavier mechanical constraints introduced by the non-edge starting point which is completely surrounded by material. As a result, the amplified difference is sufficient to lead buckling to take place in the convex direction. Once the buckling occurs in that direction, the rest of the forming process will be in that direction. The postulate is validated by the experimental and numerical results to be explained below.

Experiments

Instead of starting laser scanning from an edge (such as $X_s = 0$ in *Figure 2a*), a nonzero value of X_s was used for the reasons stated before. A scan started from a point X_s mm away from the left edge rightward till reaching the right edge. To complete the scan, the scan resumed at a point X_s mm away from the right edge leftward till reaching the left edge. The overlap in scanning was primarily to reduce the so-called edge effect.¹⁰

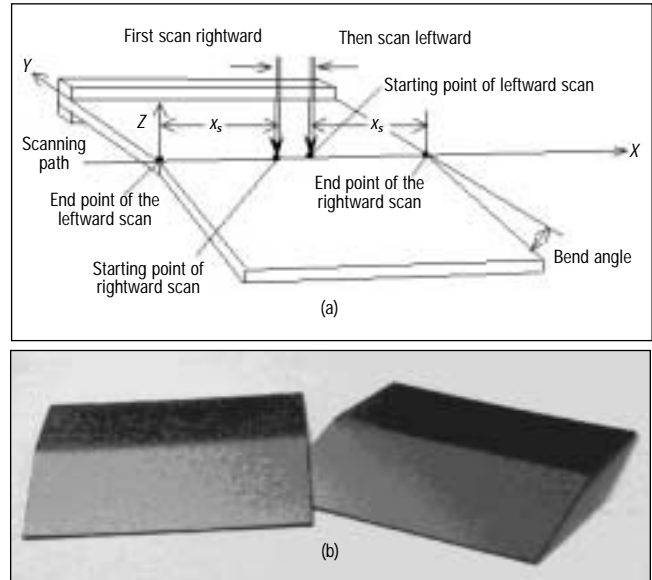


Figure 2
 (a) Scanning Scheme for Convex Laser Forming and
 (b) Samples Formed Convexly Using the Scanning Scheme

Table 1
 Experimental Parameters (sheet size: 80 x 80 mm)

No.	Power (W)	Velocity (mm/s)	Beam Diameter (mm)	Thickness (mm)
1	900	30	12.0~14.8	0.89
2	900	20~58.3	14.8	0.89
3	700	18.3~50	14.8	0.89
4	600~1010	30	14.8	0.89
5	807~1345	36.7	14.8	0.89
6	600~1200	36.7	14.8	0.61

The specimen size was 80×80 mm. Two values of thickness, 0.61 and 0.89 mm, were examined. The material was low carbon steel, AISI 1010. The sheet metal was scanned with a PRC1500 CO₂ laser system with the maximum power of 1.5 kW. The power density has a Gaussian distribution (TEM₀₀). The diameter of the laser beam is defined as the diameter at which the power density becomes $1/e^2$ of the maximum power value.

To obtain a BM-dominated laser forming process, the ratio of beam diameter to sheet thickness was kept high. The parameters used in the experiments are shown in *Table 1*.

Except for some experiments in the first group, the diameter/thickness ratio was at least equal to $14.8/0.89 = 16.6$, which ensured that the forming process will be dominated by the buckling mechanism. Typical samples so formed are shown in *Figure 2b*. The reduced diameter in the first group was to obtain conditions under which the BM may not be dominant.

The samples were first cleaned using propanol and then coated with graphite to increase coupling of laser power. During forming, the samples were clamped at one side. A coordinate measuring machine was used to measure the bending angle at different positions along the scanning path. An average bending angle was then calculated based on the measurements of the sample.

Theoretical Aspects

For an isotropic material, the relationship between stress σ_{ij} and strain ε_{ij} (including the influence of temperature) can be written in terms of tensor as:¹¹

$$\varepsilon_{ij} = \frac{1}{E} \left[(1 + \gamma) \sigma_{ij} - \gamma \delta_{ij} \sigma_{kk} \right] + \delta_{ij} \alpha \Delta T \quad (1)$$

where E is the modulus of elasticity, γ the Poisson's ratio, δ_{ij} the Kronecker delta, α the coefficient of thermal expansion, and ΔT the temperature change. In a BM-dominated laser forming process, the sheet thickness is much smaller than the laser beam size and other dimensions, and the temperature gradient is also small in the thickness direction. Therefore, the stress state that the sample undergoes can be regarded as in-plane stress state. The mechanical behavior of the sheet can be described as follows. In the discussion, axis x and y are located in the mid-plane of the sheet.

The membrane forces per unit length for a thin plate can be written in matrix form as:¹²

$$\begin{bmatrix} N_x \\ N_y \\ N_{xy} \end{bmatrix} = [\underline{A}] \begin{bmatrix} \frac{\partial u}{\partial x} \\ \frac{\partial v}{\partial y} \\ \frac{\partial u}{\partial y} + \frac{\partial v}{\partial x} \end{bmatrix} + [\underline{A}] \begin{bmatrix} \frac{1}{2} \left(\frac{\partial w}{\partial x} \right)^2 \\ \frac{1}{2} \left(\frac{\partial w}{\partial y} \right)^2 \\ \frac{\partial w}{\partial x} \frac{\partial w}{\partial y} \end{bmatrix} - [N_T] \quad (2)$$

where:

$$[\underline{A}] = \frac{Es}{1 - \gamma^2} \begin{bmatrix} 1 & \gamma & 0 \\ \gamma & 1 & 0 \\ 0 & 0 & \frac{1 - \gamma}{2} \end{bmatrix}, \quad (3)$$

$$[N_T] = \frac{E\alpha}{1 - \gamma} \int_{-\frac{s}{2}}^{\frac{s}{2}} \begin{bmatrix} \Delta T(x, y, z) \\ \Delta T(x, y, z) \\ 0 \end{bmatrix} dz$$

N_x , N_y , and N_{xy} are the membrane forces per unit length, \underline{N} is their vector representation, \underline{A} is the stiffness matrix, u and v are in-plane displacements of points on the middle surface of the plate, w is the transverse deflection, \underline{N}_T is the membrane force vector induced by a temperature change $\Delta T(x, y, z)$ from an initial temperature, and s is the plate thickness. The second term on the right-hand side of Eq. (2) is the nonlinear strain component corresponding to the transverse deflection; if assuming small transverse deflection, it can be neglected.

The deflection of the buckled plate is obtained by buckling equation:¹³

$$\nabla^4 w = \frac{1}{k} \left(N_x \frac{\partial^2 w}{\partial x^2} + 2N_{xy} \frac{\partial^2 w}{\partial x \partial y} + N_y \frac{\partial^2 w}{\partial y^2} \right) \quad (4)$$

$$k = \frac{Es^3}{12(1 - \nu^2)}$$

where k is the bending stiffness of the plate and ∇^2 is potential operator $\nabla^2 = \frac{\partial^2}{\partial x^2} + \frac{\partial^2}{\partial y^2}$. N_x , N_y , and

N_{xy} can in fact be obtained by multiplying corresponding stresses by the plate thickness and from Airy's stress function F :

$$N_x = \frac{\partial^2 F}{\partial y^2} s, \quad N_y = \frac{\partial^2 F}{\partial x^2} s, \quad N_{xy} = -\frac{\partial^2 F}{\partial x \partial y} s \quad (5)$$

The Airy's stress function F satisfies the membrane equation:

$$\nabla^4 F = -E\alpha \nabla^2 T \quad (6)$$

where T is the temperature field that the plate is subjected to. Note that Eq. (6) is equivalent to Eq. (2) if small transverse deflection is assumed.

To describe the post-buckling problem where the transverse deflection corresponding to the nonlinear term in Eq. (2) is no longer small, the Airy's stress function F has to satisfy the following von Kármán's equation:

$$\nabla^4 F = -E\alpha \nabla^2 T + E \left[\left(\frac{\partial^2 w}{\partial x \partial y} \right)^2 - \frac{\partial^2 w}{\partial x^2} \frac{\partial^2 w}{\partial y^2} \right] \quad (7)$$

For plastic thermal buckling of an isotropic homogeneous plate with the in-plane stress state, the buckling equation is:¹⁴

$$\begin{aligned} & \left(1 - \frac{3}{4}\lambda \frac{N_x^2}{\bar{N}^2}\right) \frac{\partial^4 w}{\partial x^4} + 2 \left(1 - \frac{3}{2}\lambda \frac{N_x N_y}{\bar{N}^2}\right) \frac{\partial^4 w}{\partial x^2 \partial y^2} + \\ & \left(1 - \frac{3}{4}\lambda \frac{N_y^2}{\bar{N}^2}\right) \frac{\partial^4 w}{\partial y^4} + \frac{N_x}{\bar{D}} \frac{\partial^2 w}{\partial x^2} + \\ & \frac{N_y}{\bar{D}} \frac{\partial^2 w}{\partial y^2} + 2 \frac{N_{xy}}{\bar{D}} \frac{\partial^2 w}{\partial x \partial y} = 0 \end{aligned} \quad (8)$$

$$\bar{D} = \frac{E_s s^3}{9}, \quad \lambda = 1 - \frac{E_t}{E_s} \quad (9)$$

where $E_s = \frac{\bar{\sigma}}{\bar{\epsilon}}$ is the secant modulus, $\bar{\sigma}$ the effective stress, $\bar{\epsilon}$ the effective strain, $\bar{N} = \bar{\sigma}_s$ and E_t the tangent modulus. Analytical solutions for the laser forming process are difficult to obtain without significant simplifications. Instead, numerical simulation is conducted.

Numerical Simulation

The assumptions made for the numerical modeling are as follows. Workpiece materials are isotropic. The rate of deformation is the sum of the elastic strain rate, plastic strain rate, and thermal strain rate. The heating and deformation in the laser forming is symmetrical about the laser scanning path, and the symmetric plane is assumed adiabatic. Heat generated by plastic deformation is negligible because it is small compared with heat input by the laser beam. Therefore, a sequential thermal-mechanical analysis will suffice. The laser forming process is so controlled that the maximum temperature in the workpiece is lower than the melting temperature of the sample material. No cooling of gas or water jet is followed after laser scanning.

The boundary conditions are described as follows. Heat flux generated by laser beam is only applied to top surface with a non-uniform distribution. Free heat convection with air occurs on all surfaces except the symmetric plane: $q = h(T - T_0)$, where h is the heat transfer coefficient and $T_0 = T_0(x, t)$ is the surrounding temperature. Radiation takes place on the same surfaces: $q = R((T - T_Z)^4 - (T_0 - T_Z)^4)$, where R is the radiation constant and T_Z is the absolute zero on the temperature scale used. The initial temperature is

set as 300 K. On the symmetric plane, no displacement in the Y direction occurs throughout the laser forming process.

The numerical simulation is conducted using code ABAQUS. PCL cluster function is used to create mesh seed along the Y direction so that a wider dense-mesh area using one-way bias can be obtained, which is better for BM-dominated convex laser forming process associated with large beam diameter. The same mesh is created for both thermal and structural analyses. Three-dimensional heat-transfer elements with eight nodes DC3D8 are used for thermal analysis, and continuum stress/displacement elements with the same dimension and number of nodes C3D8 are used for structure analysis. Although each scan consists of two portions, the leftward and rightward portions, the thermal and mechanical analyses are carried out sequentially. Heat flux is determined by the maximum intensity in the center of the laser beam with Gaussian distribution (TEM_{00}) and the distance of the calculating point from the laser beam center. That depends on laser beam power, absorption coefficient, beam diameter, scanning velocity, and the distance. A FORTRAN program is developed to define the magnitude of the heat flux generated by the laser beam for specific positions on the top surface of the workpiece as a user subroutine. In the model of the finite element analysis, nonlinear analysis is used because of characteristics of the forming process. The von Mises criterion is used as the yield criterion in the simulation. Temperature-dependent work hardening of the material due to plastic deformation is considered. Strain rate and temperature effects on flow stress are taken into account.¹⁵

Results and Discussion

Supporting Evidence for Postulate

Figure 3 is a histogram of bending direction for different distance from edge, X_s . When $X_s = 0$, that is, scanning from an edge, the bending direction is uncertain. This is consistent with published results; that is, in a BM-dominated laser forming process, buckling will occur, but the direction of the buckling is uncertain and heavily depends on the initial stress/strain state and surface condition. A small disturbance in favor of a particular direction will easily induce the buckling toward that direction. When X_s

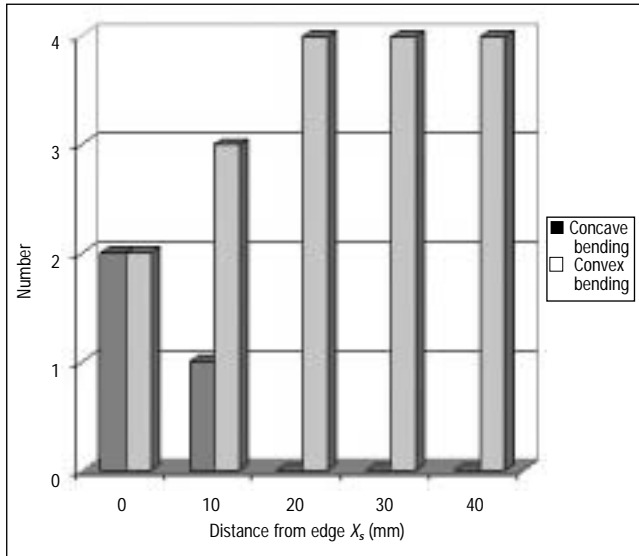


Figure 3
Histogram of Bending Direction vs. Distance from Edge, X_s
 (power: 900 W, velocity: 30 mm/s, beam diameter: 14.8 mm)

increases (the starting point of the scanning moving away from the edge), the bending becomes predominantly convex. When the starting point approaches the middle of the plate, that is, X_s approaches 40 mm, the bending is always convex. This clearly confirms the postulate made earlier; that is, even in a BM-dominated laser forming process, temperature/thermal expansion at the top surface is slightly higher than that at the bottom surface, and a slight convex bending will occur first. This is also the case in TGM-dominated processes or BM-dominated processes with the starting point of scanning at an edge. But the difference is that when the starting point is not at the edge, the initial convex bending will continue (instead of reversing) due to the added mechanical constraints of the surrounding materials. As a result, the rest of the forming process will understandably follow its lead. More discussions will be given later in the paper when transient simulation results are discussed. For the rest of the experiments and all simulation studies, $X_s = 25$ mm.

Effect of Fourier Number

The Fourier number, F_o , is defined as $F_o = \frac{\alpha_d d}{s^2 V_s}$, where α_d is the thermal diffusivity, d the beam diameter, s the sheet thickness, and V_s the scanning velocity. d/V_s is the time that a point on the surface on the center line of the scan is exposed to the laser, and s^2/α_d is the characteristic time for heat to propagate through the sheet. It has been known that a smaller

value of the Fourier number corresponds to a TGM-dominated laser forming process, while a larger value corresponds to a BM-dominated process. Shown in *Figure 4* are experimental and simulated bending angles at both convex and concave directions when the Fourier number F_o varies from about 6.25 to 7.75. The variation in F_o is obtained by varying the laser beam diameter from 12 to 14.8 mm while keeping other parameters unchanged (the first group in *Table 1*). It can be seen that corresponding to small values of the Fourier number, concave bending, represented by a positive value, always occurs evenly ($X_s = 25$ mm). That is, because the temperature gradient along the thickness direction is higher and TGM plays a dominant role. The added mechanical constraints by moving the starting point away from an edge have little effect here.

When F_o increases, the direction of bending becomes uncertain. As seen for $F_o = 6.6$ to 6.8, the bending is sometimes convex (represented by negative bending angles) and sometimes is concave. Obviously, in this region, neither TGM nor BM dominates. Beyond the critical region, convex bending always takes place for the reasons already stated earlier. It has been known that the Fourier number can be used as the criterion to determine whether a laser forming process is TGM or BM dominant. *Figure 4* shows that F_o can be reliably used as a criterion to predict concave and convex bending under the new scanning scheme used (e.g., nonzero X_s). The switch between concave and convex forming will be further discussed with the simulation results that follow.

Simulation Validation

Simulation results of bending direction and angle are superposed on experimental results in *Figure 4*, and a good agreement can be seen. It should be noted that, unlike experimental results, the simulation curve shows a sharp switch from the concave and convex bending when the Fourier number increases because the uncertainties existing in the experiments do not exist in simulation. A typical result of thermal-mechanical simulation of convex laser forming is shown in *Figure 5*. *Figure 5a* shows temperature distribution and deformation when a laser beam is scanning through the workpiece. Only half of the plate is shown due to symmetry. Please note the deformation is magnified to show the workpiece bends convexly in the early stage of the form-

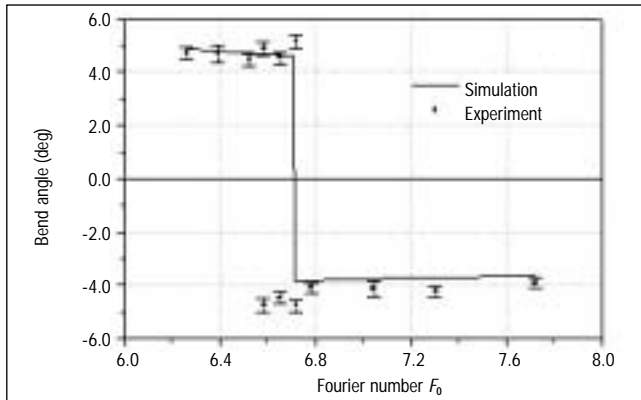


Figure 4

Bend Angle vs. Fourier Number, F_0
 (power: 900 W, velocity: 30 mm/s, dimension: $80 \times 80 \times 0.89$ mm,
 diameter: 12-14.8 mm)

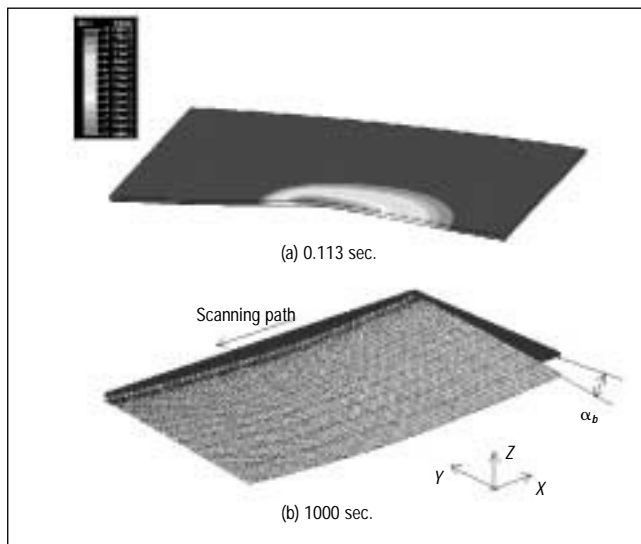


Figure 5

(a) Deformed Shape with Temperature Contour
 (deformed magnification 5X) and
 (b) Comparison Between Undeformed Sample (Top)
 and Deformed One (Bottom), Deformed Magnification 3.5X,
 Showing Half Plate Due to Symmetry
 (power = 800 W, velocity: 30 mm/s, beam diameter: 14.8 mm,
 workpiece size: $80 \times 80 \times 0.89$ mm)

ing process. Figure 5b shows a formed sheet that has undergone natural cooling for quite a few minutes. Comparing it with the undeformed sheet shown in the same figure, it is obvious that it is convexly bent. It can also be seen that the bending edge is curved (although magnified), and this is because the X-axis plastic contraction near the top surface is larger than that near the bottom surface.¹⁰

Shown in Figure 6 are comparisons between numerical and experimental results of bending angle vs. power and nondimensional velocity V_n .¹⁶ For obvious reasons, the bending angle becomes more

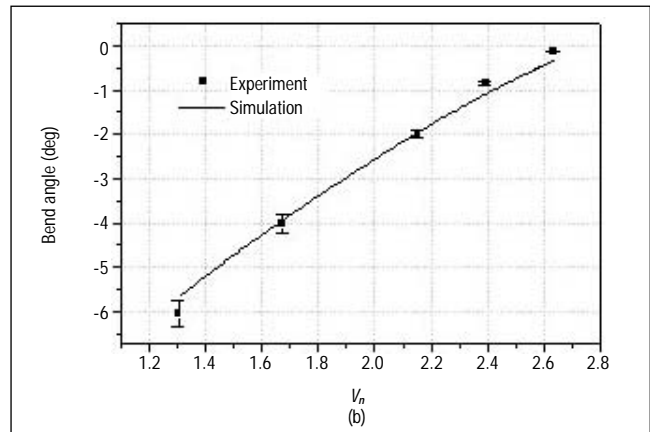
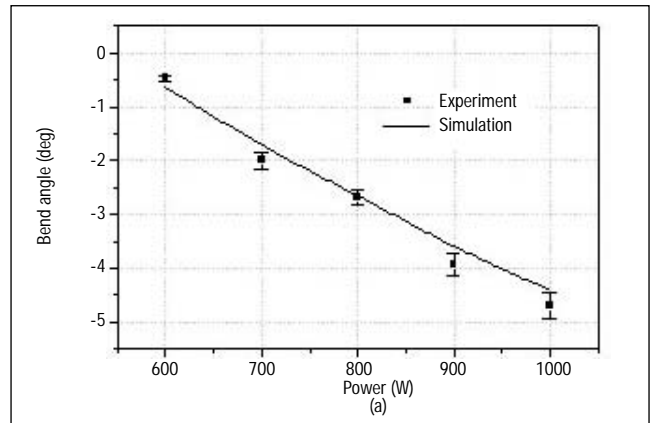


Figure 6

Numerical and Experimental Results of Variation of
 Bend Angle with Power p
 (a) scanning velocity: 30 mm/s and dimensionless velocity v_n
 and (b) power: 700 W, beam diameter: 14.8 mm,
 workpiece size: $80 \times 80 \times 0.89$ mm

negative (larger convex bending) with laser power increase. V_n , defined as $V_s/s/\alpha_d$, is the ratio between the laser scanning velocity V_s and the characteristic velocity $s/(s^2/\alpha_d)$ for heat to propagate through the sheet thickness, where s^2/α_d is the characteristic time for heat to propagate through the sheet thickness. This means a larger V_n does not promote buckling, which requires more uniform heat up throughout the thickness, and as a result, the bending is less negative (e.g., smaller convex bending). Figures 4 and 6 together show that the simulation results are fairly consistent with the experimental measurements.

Parametric Analysis

Figure 7 shows the relationship between bend angle and dimensionless velocity V_n at two different power levels. It is obvious that as V_n increases, the absolute value of the bending angle reduces. A threshold value of V_n can be seen, above which no

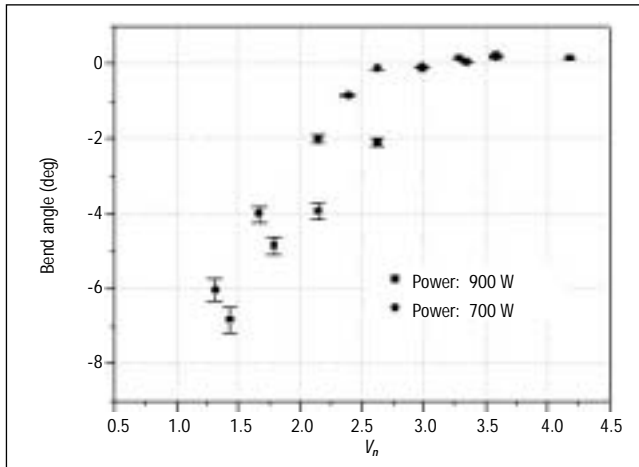


Figure 7

Bend Angle vs. Dimensionless Velocity, v_n
 beam diameter: 14.8 mm, sample dimension: 80 × 80 × 0.89 mm

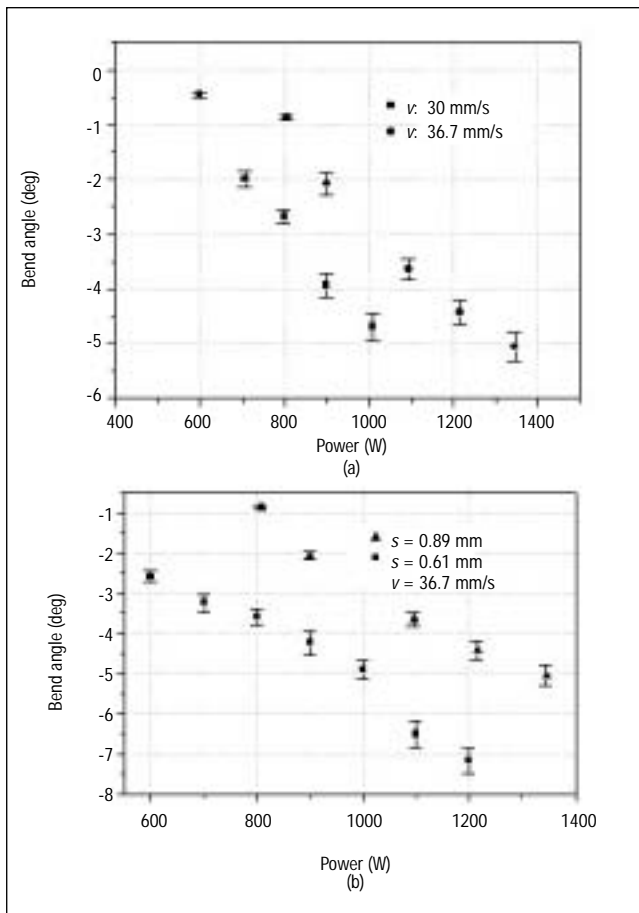


Figure 8

Bend Angle vs. Power (a) At Different Scanning Velocities
 (sheet thickness: 0.89 mm) and (b) At Different Levels of Thickness
 (both beam diameter: 14.8 mm and sample size: 80 × 80 mm)

on laser power under two different velocities. As seen, the higher the power, the larger the absolute value of the bending angle due to obvious reasons. Shown in *Figure 8b* is bending vs. power under two different values of thickness. Again the trends are readily understood. These results are of course different from the condition of constant line energy.¹⁷

More Discussions on Convex Forming Mechanism

To obtain further insights into the reasons that the convex forming is always obtained when the starting point of laser scanning moves from an edge to a point closer to the center of the sheet, the transient plots from simulation are shown in *Figure 9*. The plots are for the starting point $X_s = 25$ mm. At time = 0 sec., the scan begins at the starting point rightward, proceeds till it passes the right edge, and waits there for quite a few minutes for the sheet to cool down before completing the scan leftward (*Figure 2a*). Shown in *Figure 9* is the time history of the first 100 seconds.

Figure 9a confirms that, although small, there is a temperature difference between the top and bottom surface under the process condition, which is known to induce the buckling mechanism (BM). As a result, there is slightly more thermal expansion at the top surface than that at the bottom surface, resulting in a small negative bending angle (convex bending), as seen from *Figure 9b*. The small convex bending angle in turn causes a slightly more compressive stress at the bottom than that at the top, as seen from *Figure 9c*. This trend continues till about $t = 0.7$ sec. At that point, the convex bending angle has grown big enough to make the buckling happen, of course, in the same direction, which is the convex direction. This is evident in the dramatic increase in the negative bending angle within a fraction of a second (from about 0.7 to 1.1 sec., as seen from *Figure 9b*). As a result, the compressive stress at the top surface also abruptly reverses its sign to become tensile (*Figure 9c*).

It should be pointed out that the initial small convex bending angle exists in laser forming under almost any condition. This includes TGM-dominated processes. This also includes BM-dominated processes in which the starting point of the laser scan is from an edge of the workpiece. In the TGM-dominated processes, the small convex bending angle is quickly reversed to a large concave bending angle because the significant shortening at the top

bending takes place due to insufficient induction of buckling and also due to insufficient energy input. Shown in *Figure 8a* is dependence of the bend angle

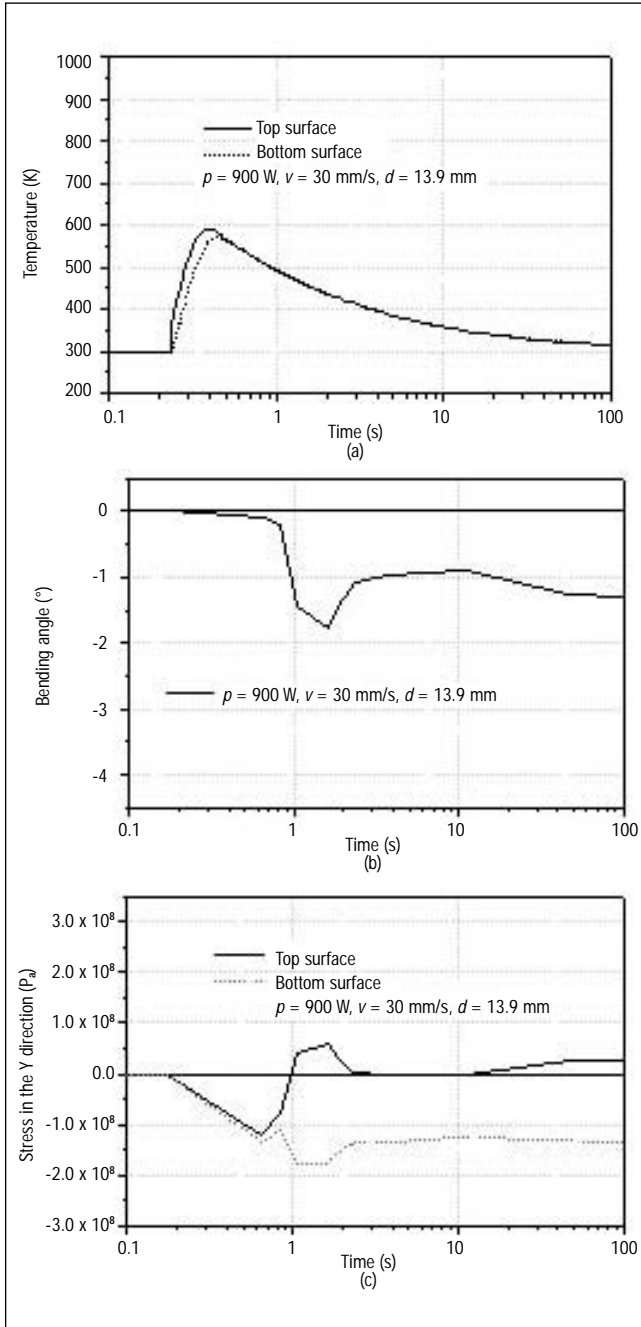


Figure 9
 Typical Time History of (a) Temperature, (b) Bend Angle, and (c) Y-Axis Stress at the Starting Point, $X_s = 25$ mm ($p = 900$ W, $v = 30$ mm/s, $d = 13.9$ mm, workpiece $80 \times 80 \times 0.89$ mm)

surface caused by significant temperature gradient through the thickness serves as a strong pulling force during cooling. In the BM-dominated processes in which the starting point of the laser scan is from an edge of the workpiece, the initial small convex bending angle may lead to either direction. This is because the mechanical constraints near the edge

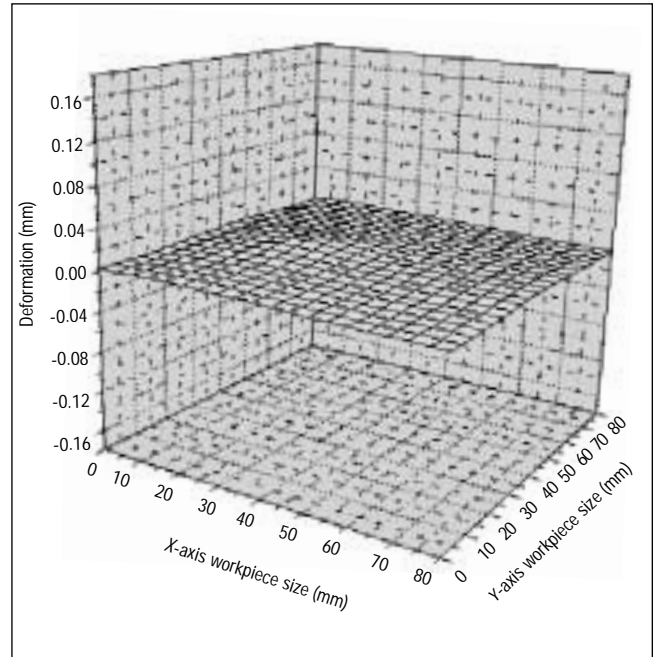


Figure 10
 Deformation at $X_s = 25$ mm Caused by Laser Irradiation (both laser and workpiece stationary, laser duration: 300 ms, beam diameter: 14.8 mm, power: 700 W, dimension: $80 \times 80 \times 0.89$ mm)

are less. As a result, the inducing effect of the initial convex bending angle can be easily overturned by other forms of small disturbances, such as the sheet and surface condition or pre-strain condition at the location.

But this is not the case for the conditions used in this paper. Once an initial small convex bending angle is formed, it is very hard, if not impossible, to reverse because of the heavier mechanical constraints surrounding the starting point. As a result, the buckling can only take place in the same direction as the initial direction, that is, the convex direction. In addition, due to the heavier constraint in the case of starting at a non-edge location, the initial small convex bending can be up to 50% larger than that when starting at an edge, while all other conditions are kept the same. This again makes it more difficult to reverse the initial convex bending. To further illustrate the point, a laser beam was momentarily irradiated at $X_s = 25$ mm while both the laser and workpiece were kept stationary. The caused deformation was measured and plotted in *Figure 10*. The deformation in the Z-direction at the location was measured as 0.011 mm, which is about 40% larger than that if the irradiation took place at an edge ($X_s = 0$ mm), obviously because of less mechanical constraints to deformation at the edge.

Conclusion

A new scanning scheme is postulated in which laser scanning starts from a location near the middle of the workpiece instead of normally from an edge of the workpiece. Using the scanning scheme, convex forming is realized with high certainty, unlike the case of scanning from the edge. The postulation is based on the analysis that the added mechanical constraints, by moving the starting point from an edge to the middle, will sustain the initial convex deformation, which exists in both concave and convex forming. The postulate is successfully validated by experimental and numerical results. With the method, neither pre-bending nor additional external mechanical constraints are needed to effect convex laser forming.

The underlying physical phenomena, including temperature, stress, and strain near the starting point, are comparatively investigated to give a better understanding of the forming mechanisms and effects of the new and conventional scanning schemes. Even with the new scanning scheme, the certain condition of process parameters still needs to be satisfied. Otherwise, convex forming may not be reliably attained or not be attainable at all. In this connection, the Fourier number F_o can still be used as a threshold between the concave and convex deformation, as it has been used in laser forming to date to distinguish between TGM and BM-dominated forming processes.

References

1. F. Vollertsen, "Mechanism and Models for Laser Forming," Proc. of LANE'94 (v1, 1994a), pp345-360.
2. F. Vollertsen, M. Geiger, and W.M. Li, "FDM and FEM Simulation of Laser Forming a Comparative Study," Adv. Technology of Plasticity (v3, 1993), pp1793-1798.

3. Y.-C. Hsiao, H. Shimizu, L. Firth, W. Maher, and K. Masubuchi, "Finite Element Modeling of Laser Forming," Proc. of ICALEO'97, Section A, pp31-40.
4. N. Alberti, L. Fratini, and F. Micari, "Numerical Simulation of the Laser Bending Process by a Coupled Thermal Mechanical Analysis," Proc. of LANE'94 (v1), pp327-336.
5. N. Alberti, L. Fratini, and F. Micari, M. Cantello, and G. Savant, "Computer Aided Engineering of a Laser Assisted Bending Process," Proc. of LANE'97 (v2), pp375-382.
6. A.K. Kyrsanidi, T.B. Kermanidis, and S.G. Pantelakis, "Numerical and Experimental Investigation of the Laser Forming Process," Journal of Materials Processing Technology (v87, 1999), pp281-290.
7. H. Arnet and F. Vollertsen, "Extending Laser Bending for the Generation of Convex Shapes," IMechE Part B: Journal of Engg. Manufacture (v209, 1995), pp433-442.
8. S. Holzer, H. Arnet, and M. Geiger, "Physical and Numerical Modeling of the Buckling Mechanism," Proc. of LANE'94 (v1), pp379-386.
9. F. Vollertsen, I. Komel, and R. Kals, "The Laser Bending of Steel Foils for Microparts by the Buckling Mechanism—A Model," Modeling and Simulation in Materials Science and Engg. (v3, 1995), pp107-119.
10. J. Bao and Y.L. Yao, "Analysis and Prediction of Edge Effects in Laser Bending," Proc. of ICALEO'99, San Diego, CA.
11. B.A. Boley and J.H. Weiner, Theory of Thermal Stresses (Mineola, NY: Dover Publications, 1997).
12. E.A. Thornton, J.D. Kolenski, and R.P. Marino, "Finite Element Study of Plate Buckling Induced by Spatial Temperature Gradients," 34th AIAA/ASME/ASCE/AHS/ASC Structures, Structural Dynamics and Materials Conf., La Jolla, CA, 1993, pp2313-2326.
13. E.A. Thornton, M.F. Coyle, and R.N. McLeod, "Experimental Study of Plate Buckling Induced by Spatial Temperature Gradients," Journal of Thermal Stresses (v17, 1994), pp191-212.
14. N.G.R. Iyengar, Structural Stability of Columns and Plates (West Sussex, UK: Ellis Horwood, 1988).
15. W. Li and Y.L. Yao, "Effects of Strain Rate in Laser Forming," Proc. of ICALEO'99, San Diego, CA.
16. Z. Mucha, J. Hoffman, and W. Kalita, "Laser Forming of Thick Free Plates," Proc. of LANE'97, pp383-392.
17. W. Li and Y.L. Yao, "Laser Forming With Constant Line Energy," accepted Int'l Journal of Advanced Mfg. Technology, 1999b.

Authors' Biographies

Dr. Wenchuan Li was a PhD candidate and is currently with Ford Motor Co.

Y. Lawrence Yao is an associate professor with research interest in manufacturing and design, laser machining, laser forming, and laser shock processing.